APPLIED PHYSICS LETTERS **101**, 123110 (2012)

Tunable electroluminescence from polymer-passivated 3C-SiC quantum dot thin films

B. Xiao,[1] X. L. Wu,[1,a)] W. Xu,[2] and Paul K. Chu[3,a)]
[1]*National Laboratory of Solid State Microstructures and Department of Physics, Nanjing University, Nanjing 210093, People's Republic of China*
[2]*National Laboratory of Solid State Microstructures and School of Electronic Science and Engineering, Nanjing University, Nanjing 210093, People's Republic of China*
[3]*Department of Physics and Materials Science, City University of Hong Kong, Tat Chee Avenue, Kowloon, Hong Kong*

(Received 14 May 2012; accepted 5 September 2012; published online 19 September 2012)

Strong room-temperature photoluminescence in the wavelength range of 400-540 nm is achieved from a thin film containing polymer encapsulated 3*C*-SiC quantum dots (QDs). The QD surface is completely passivated by the polymer so that the QD film possesses voltage-tunable electroluminescence. The electroluminescence spectrum blue-shifts from 490 to 460 nm when the applied voltage is increased from 5 to 10 V. The tunable electroluminescence is attributed to carrier recombination in the core quantum confinement states as a result of Pool-Frenkel emission. Owing to the environmental friendliness, nontoxicity, easy fabrication, and stability, the polymer passivated 3*C*-SiC QD thin films have promising applications. © *2012 American Institute of Physics*. [http://dx.doi.org/10.1063/1.4753995]

Semiconductor nanocrystals (NCs) or quantum dots (QDs) have attracted much interest because of potential optoelectronic applications such as solar cells,[1–3] bistable memory devices,[4–6] and photodetectors.[7] The unique properties of inorganic QDs such as high luminescence efficiency, broad wavelength tunability, saturated color emission, and photochemical stability make them very attractive to hybrid QD-organic light-emitting diodes (QD-OLEDs).[8–19] Most of these QD materials are composed of group II–VI semiconductors such as CdSe, CdZnSe, ZnSe, or CdZnS with single or multiple shells. These QD materials have heavy metal cations such as cadmium or lead and the synthesis procedures are generally quite complex. Tu *et al.*[20] have replaced II-VI QDs by heavy metal free Si QDs that are also potentially compatible with Si processing technology. However, the complex sandwiched structure in the Si QD-OLEDs suffers from leakage current because of poor structural stability such as particle aggregation and QD grain boundaries in the active layer.

Silicon carbide (SiC) is a promising material in biophysical and biomedical applications due to its small weight, strength, hardness, wear and corrosion resistance, and inertness. SiC nanostructures have recently attracted considerable interest because of the quantum-confined optical emission[21,22] and applications to fluorescent biological labels.[23] SiC QDs show tunable band gaps when the dot size is close to the Bohr exciton radius of bulk SiC (2.7 nm). Furthermore, SiC QDs are environmentally friendly and nontoxic compared to II–VI QDs. However, stable and tunable photoluminescence (PL) and electroluminescence (EL) from SiC QD solid films have not been accomplished due to easily formed surface Si and C-related non-radiative centers.[21] This situation will be easier to take place if 3C-SiC QDs are embedded in silicon oxide matrix. Wang *et al.*[24] produced glycerol-bonded 3*C*-SiC QD solid films exhibiting strong and tunable violet to blue-green (360–540 nm) emission as a result of the quantum confinement effects rendered by 3*C*-SiC QDs. However, the films are not suitable for EL devices because of strong hydrophilicity of the glycerol molecules. In this letter, we report a unique process to produce a thin film comprising polymer passivated 3*C*-SiC QDs. The materials exhibit strong PL from blue to green (400–520 nm) due to the quantum confinement on 3C-SiC QDs and voltage-tunable EL can also be achieved.

The fabrication procedures for the water suspension containing the 3*C*-SiC QDs have been described previously.[25] The suspension contains 3*C*-SiC QDs smaller than 7 nm and they have -OH and -H functional groups on the Si-terminated surface.[26,27] Poly (acrylic acid) (PAA) chains are bonded to the H-terminated 3*C*-SiC QD surface via a self-addition reaction under blue ($\lambda_{\text{blue}} = 490$ nm) and ultraviolet (UV) ($\lambda_{\text{UV}} = 360$ nm) irradiation.[28] In a typical process, 2 ml of 98 wt. % monomer acrylic acid and 20 ml of 99.7 wt. % ethanol were introduced into 8 ml of the 3*C*-SiC QD suspension (QD concentration = 2 mg/ml). The mixture was purged with N_2 for 30 min to remove dissolved oxygen and then irradiated with blue light for 1 h while magnetically stirred. The acrylic acid monomers reacted with the 3*C*-SiC QDs to form surface Si-O bonds. Afterwards, UV irradiation was conducted for an hour or longer to initiate the hydrosilylation reaction and additional reaction to form the PAA chains. Under UV irradiation, the alkene in the polymer chain and residual acrylic acid monomers reacted to produce the PAA with a high degree of polymerization and then a colloid containing the QDs-PAA complex. After cooling, the liquid was transferred to a dialysis bag to remove the residual acrylic acid and ethanol. After drying for several hours, a sticky colloid was obtained, put onto a flat substrate such as a silicon wafer, and dried to form the thin film containing the polymer encapsulated 3*C*-SiC QDs. The film served as the luminescent active layer in the EL device.

[a)] Authors to whom correspondence should be addressed. Electronic addresses: hkxlwu@nju.edu.cn and paul.chu@cityu.edu.hk.

0003-6951/2012/101(12)/123110/4/$30.00

Commercial indium tin oxide (ITO) coated glass with a sheet resistance of 20 Ω/□ was washed with a detergent and rinsed with de-ionized water, acetone, and isopropyl alcohol sequentially in an ultrasonic bath for 5 min. A thin film containing the polymer encapsulated 3*C*-SiC QDs (∼50 nm thick) was spin-coated at 4000 rpm for 40 s onto the ITO surface and then dried at 70 °C for 2 h. An Al cell array (∼400 nm thick) was thermally evaporated onto the film and served as the top electrode. The morphology of the QDs was examined by high-resolution transmission electron microscopy (HR-TEM; JEM-2010, 200 kV). Fourier transform infrared (FTIR) spectra were obtained on a NEXUS870 FTIR spectrometer and x-ray photoelectron spectroscopy (XPS) was carried out on a PHI5000 VersaProbe XPS spectrometer. The PL spectra were taken on a FluoroMax-2 fluorescence spectrometer with a resolution limit of 1 nm. The excitation source (Xe lamp) intensity was calibrated carefully. The current-voltage (I-V) characteristics of the device were measured under forward biasing conditions using a HP4156C semiconductor parameter analyzer and the EL spectra were acquired using the standard CCD detector under a negative DC voltage applied to the top surface electrode. All the EL spectra were corrected for the quantum efficiency of CCD detector. The light emission was monitored by an optical power meter and all the measurements were performed at room temperature.

Fig. 1(a) depicts the TEM image of the as-prepared 3*C*-SiC QDs that are nearly spherical and have diameters between 1.5 and 6.5 nm. The HR-TEM image of a representative QD is shown in Fig. 1(b). The QD is highly crystalline and the lattice fringes correspond to the (111) plane of 3*C*-SiC. Fig. 1(c) displays the histogram of the QD size distribution revealing an almost asymptotic centric distribution and the diameters of most QDs are between 2 and 4 nm. The Gaussian fit shows that the most probable QD diameter is about 3.3 nm.

To confirm bonding between the polymer and 3*C*-SiC QDs and simultaneously investigate the surface structures, the FTIR spectrum is presented in Fig. 2(a). With the exception of the strong SiC optical phonon at 813 cm^{-1},[26] all the peaks are associated with the QD surface and polymer. The strong peaks around 1700 and 1200 cm^{-1} are attributed to C═O and C-O vibrations, and the weak peaks at around 1450 and 1100 cm^{-1} are associated with C-O and Si-O vibrations,[29] respectively. The signal at around 2900–3000 cm^{-1} indicates C—H stretching in CH_n (n = 1-3).[26,30] No characteristic Si–H stretching bands can be observed in the range between 2100 and 2200 cm^{-1},[30] indicating that the Si-H bonds on the QD surface have been replaced by other bonds of the polymer.

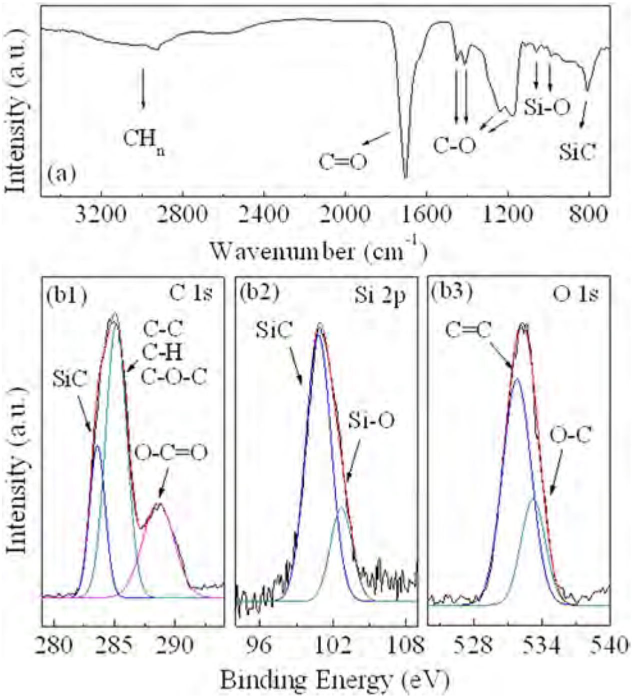

FIG. 2. (a) FTIR and (b1-b3) C 1s, Si 2 p, and O 1s core level XPS spectra of the thin film containing the polymer-encapsulated 3C-SiC QDs deposited on a c-Si substrate.

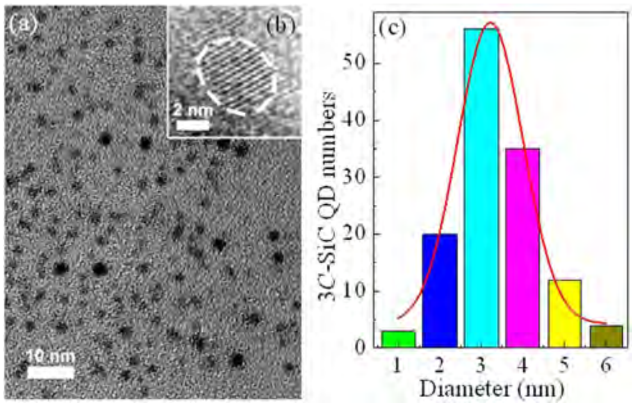

FIG. 1. (a) TEM image of the as-fabricated 3C-SiC QDs. (b) High-resolution TEM image of a QD with lattice fringes corresponding to the (111) plane of 3C-SiC. (c) QD number distribution showing the most probable size of 3.3 nm determined by Gaussian fitting.

Fig. 2(b) shows the C 1s, Si 2 p, and O 1s core level XPS spectra of the QD film. In the C 1s spectrum, the peak at 283.1 eV corresponds to SiC.[24,31,32] The strong peak at around 285 eV can be attributed to the combined signal of C-C, C-H, and C-O-C[31–33] and the weak peak at 289 eV can be ascribed to C-O═C.[33] In the Si 2 p spectrum, the low-energy peak corresponds to SiC and that at 102.8 eV is associated with Si-O-C.[31] The 531.6 and 533.2 eV peaks in the O 1s spectrum arise from C═O and C-O,[34] respectively. The FTIR and XPS results are consistent with the PAA chain structure on the QD surface.[28] The PAA chains which have long alkyl chains with many carboxyl branches bond to the QD via Si-C and Si-O bonds. By means of shell approximation,[26,35] the number of atoms in the QD is calculated to be $N_{\text{SiC}} = 4\pi d^3/3a^3$, where *d* and *a* are the QD diameter and lattice constant (0.436 nm for 3*C*-SiC), respectively. The QD with a diameter of 3.3 nm has approximately 1800 atoms and the number of silicon and carbon is almost the same at 900. The Si/O atomic ratio is about 1:3 based on the areas shown in the C 1s spectrum and the C/O atomic ratio (3:2 for acrylic acid) is about 2:1. The QD core with a polymer shell has approximately 9000 atoms. It has a diameter of 5.6 nm if it is assumed to be totally 3*C*-SiC. Considering that the bond length of Si-C is longer than that of C-C, the SiC core has a diameter of 3.3 nm and the thickness of the polymer shell is about 1 nm thick. The results indicate complete surface passivation of the 3*C*-SiC QD surface by the polymer.

Fig. 3 shows the PL spectra acquired from the thin film composed of the polymer encapsulated 3*C*-SiC QDs excited

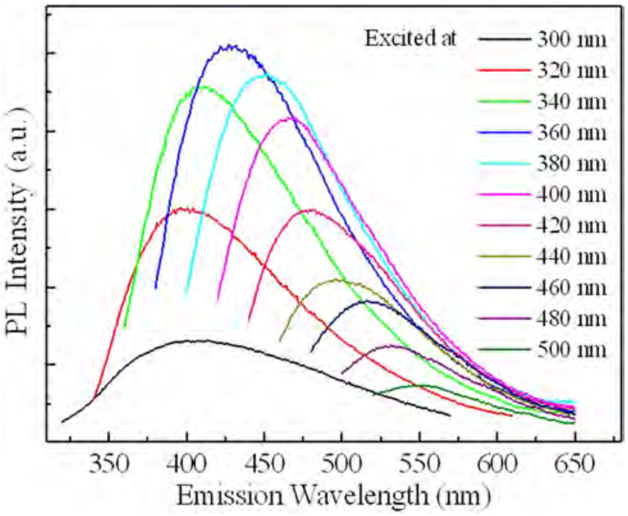

FIG. 3. PL spectra of the thin film containing the polymer-encapsulated 3C-SiC QDs excited by different wavelengths.

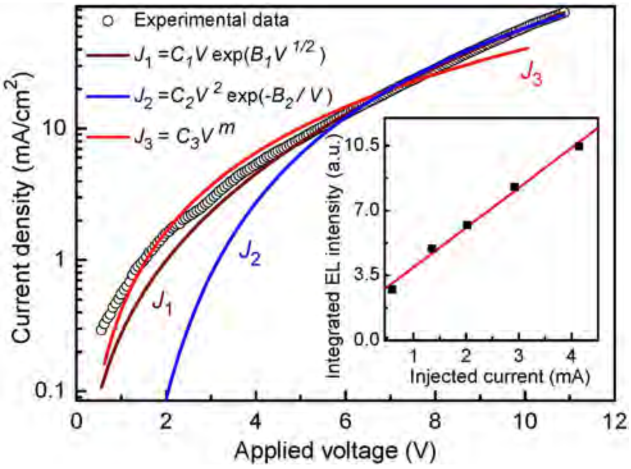

FIG. 4. $J-V$ characteristics of the devices under forward biasing with the experimental data fitted by $J_1 = C_1 V \exp(B_1 V^{1/2})$ for PF emission, $J_3 = C_3 V^m$ for SCLC, and $J_2 = C_2 V^2 \exp(-B_2/V)$ for FN tunneling (Refs. 36 and 37). The inset shows the plots of the integrated EL intensity as a function of injection current for the device.

by the 300 to 500 nm lines of a Xe lamp. The PL is so intense that the emission spots can be observed visually. As the excitation wavelength is increased from 300 to 500 nm, the PL peak position increases monotonically from 400 to 540 nm. The PL red-shift with increasing excitation wavelength can be attributed to the quantum confinement effect in lieu of defects/surface states.[21,24] The 510 nm band is not observed because of the absence of H$^+$ and OH$^-$ structures on the surface of the QDs.[26] The variety of the PL peak intensity is related of QDs' size distribution. The intensity of the PL peak centered at about 430 nm reaches a maximum at an excitation wavelength of 360 nm. For the most probable QD diameter, the largest PL intensity is derived to be at ∼428 nm (∼2.9 eV),[21,24,25] which is in good agreement with the experimental value. When the excitation wavelength increases from 300 to 360 nm, the number of the excited QDs with appropriate sizes increases. Consequently, the PL intensity in this range increases with excitation wavelength. When the excitation wavelength exceeds 360 nm, the number of 3*C*-SiC QDs that can be excited diminishes, as manifested by the continuous decrease in the PL intensity. When the excitation wavelength is larger than 480 nm, only a few QDs can be excited and the PL intensity is low. When the excitation wavelength is 500 nm, the PL intensity decreases rapidly, because when the excitation energy is close to the band gap of bulk 3*C*-SiC (2.24 eV), the QDs can hardly be excited.

Fig. 4 shows the current density vs voltage $(J-V)$ curve obtained from the corresponding device. To explain the charge transport behavior, different conduction models such as Fowler–Nordheim (FN) tunneling, Poole-Frenkel (PF) emission, and space charge-limited current (SCLC) are usually adopted for Si-based materials.[36,37] In the present case, the experimental data acquired at the applied voltages of >4 V (turn-on voltage) can be fitted very well by $J_1 = C_1 V \exp(B_1 V^{1/2})$ (The fit is a bit off in the 0 to 4 V region probably because the current threshold is not reached). This relationship is well known as the PF emission,[37] indicating that the carrier transport process is governed by PF emission.

The EL spectra at applied voltages between 5 and 10 V at room temperature are shown in Fig. 5(a). When the applied voltage is increased from 5 to 10 V, the EL peak blue-shifts from 490 to 460 nm. The EL device has a low

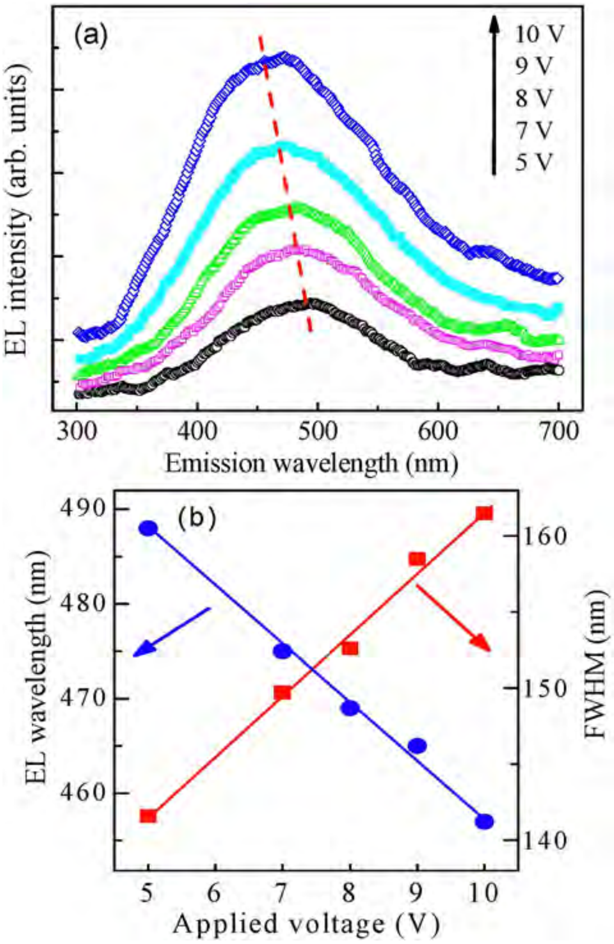

FIG. 5. (a) EL spectra of the 3C-SiC QD-based device acquired at different applied voltages with the dashed line showing the blue-shift. (b) Central wavelength and FWHM of the EL spectra as a function of the applied voltage.

turn-on voltage of 4−5 V. No EL signal is observed in the <4 V region because the current threshold is not reached. We also found that the breakdown voltage of the QD film is ~11 V. At a higher voltage (>11 V), no EL is observed. In Fig. 5(b), we plot the different central wavelengths and full-width at half maximum (FWHM) as a function of the applied voltage. A good linear dependence can be observed, indicating that the EL is closely related to the QD excitation with different sizes. The inset in Fig. 4 reveals a linear relationship between the integrated EL intensity and injected current, implying that the EL arises mainly from radiative recombination of electron-hole pairs at the luminescent centers in which the 3C-SiC QDs with different sizes are responsible for the tunable EL. From these results above, we can describe the mechanism of the EL blueshift as follows. The Poole-Frenkel emission describes an electrically assisted thermionic emission in the bandgap. Electrons do not need as much thermal energy to get into the conduction band since part of this energy comes from being pulled by the electric field. The EL emission can be attributed to electron-hole recombination in the core quantum confinement states. Because of the quantum confinement, reduction in the QD sizes widens the bandgap. Thus, at a low applied voltage, electrons can get into the conduction band of large QDs due to the narrow bandgap and the EL has a large wavelength. The EL peak blue-shifts when small QDs are excited by a higher voltage. Emission from smaller QDs dominates the EL spectra as the applied voltage is increased further (large-size QDs are still excited at a high applied voltage due to the narrow bandgap). This leads to the EL peak to be asymmetrical (consistent with the PL feature), especially at an applied voltage of 10 V. After the applied voltage exceeds 11 V, the film is broken down. This makes many smaller QDs unable to be excited and thus the EL spectral range looks narrower than the PL spectral distribution.

In summary, a robust and stable thin film containing polymer encapsulated 3*C*-SiC QDs is produced. FTIR and XPS reveal complete surface passivation of the 3*C*-SiC QDs by the polymer and tunable PL is observed from the film at room temperature. When the excitation wavelength is increased from 300 to 500 nm, the PL peak position changes from 400 to 540 nm due to the quantum confinement effects rendered by the 3*C*-SiC QDs. The EL device fabricated using the materials exhibits voltage-tunable EL. The EL spectrum blue-shifts from 490 to 460 nm when the applied voltage is increased from 5 to 10 V on account of carrier recombination in the core quantum confinement states and the current transport is due to a PF emission.

This work was jointly supported by National Basic Research Program of China (2011CB922102), National Natural Science Foundation of China (60976063), and PAPD. Partial support was also from the Hong Kong Research Grants Council (RGC) under General Research Funds (GRF) No. CityU 112510.

[1] H. C. Leventis, S. P. King, A. Sudlow, M. S. Hill, K. C. Molloy, and S. A. Haque, Nano Lett. **10**, 1253 (2010).
[2] F. Li, D. I. Son, S. H. Cho, W. T. Kim, and T. W. Kim, Nanotechnology **20**, 155202 (2009).
[3] I. Gur, N. A. Fromer, M. L. Geier, and A. P. Alivisatos, Science **310**, 462 (2005).
[4] J. Y. Ouyang, C. W. Chu, C. R. Szmanda, L. P. Ma, and Y. Yang, Nature Mater. **3**, 918 (2004).
[5] J. H. Jung, J. Y. Jin, I. Lee, T. W. Kim, H. G. Roh, and Y. H. Kim, Appl. Phys. Lett. **88**, 112107 (2006).
[6] D. Y. Yun, J. M. Son, T. W. Kim, S. W. Kim, and S. W. Kim, Appl. Phys. Lett. **98**, 243306 (2011).
[7] S. A. McDonald, G. Konstantatos, S. G. Zhang, P. W. Cyr, E. J. D. Klem, L. Levina, and E. H. Sargent, Nature Mater. **4**, 138 (2005).
[8] Q. J. Sun, Y. A. Wang, L. S. Li, D. Y. Wang, T. Zhu, J. Xu, C. H. Yang, and Y. F. Li, Nat. Photonics **1**, 717 (2007).
[9] A. Rizzo, M. Mazzeo, M. Biasiucci, R. Cingolani, and G. Gigli, Small **4**, 2143 (2008).
[10] P. O. Anikeeva, J. E. Halpert, M. G. Bawendi, and V. Bulovic, Nano Lett. **9**, 2532 (2009).
[11] W. K. Bae, J. Kwak, J. W. Park, K. Char, C. Lee, and S. Lee, Adv. Mater. **21**, 1690 (2009).
[12] G. Cheng, M. Mazzeo, S. Carallo, H. P. Wang, Y. G. Ma, and G. Gigli, Appl. Phys. Lett. **97**, 103107 (2010).
[13] F. S. Li, T. L. Guo, and T. W. Kim, Appl. Phys. Lett. **97**, 062104 (2010).
[14] A. K. Rath, S. Bhaumik, and A. J. Pal, Appl. Phys. Lett. **97**, 113502 (2010).
[15] Y. Q. Zhang and X. A. Cao, Appl. Phys. Lett. **97**, 253115 (2010).
[16] E. M. Likovich, R. Jaramillo, K. J. Russell, S. Ramanathan, and V. Narayanamurti, Adv. Mater. **23**, 4521 (2011).
[17] L. Qian, Y. Zheng, J. G. Xue, and P. H. Holloway, Nat. Photonics **5**, 543 (2011).
[18] Z. N. Tan, Y. Zhang, C. Xie, H. P. Su, J. Liu, C. F. Zhang, N. Dellas, S. E. Mohney, Y. Q. Wang, J. K. Wang, and J. Xu, Adv. Mater. **23**, 3553 (2011).
[19] R. W. Xuan, J. P. Xu, X. S. Zhang, P. Li, C. Y. Luo, Y. Y. Wu, and L. Li, Appl. Phys. Lett. **98**, 041907 (2011).
[20] C. C. Tu, L. Tang, J. D. Huang, A. Voutsas, and L. Y. Lin, Appl. Phys. Lett. **98**, 213102 (2011).
[21] X. L. Wu, J. Y. Fan, T. Qiu, X. Yang, G. G. Siu, and P. K. Chu, Phys. Rev. Lett. **94**, 026102 (2005).
[22] J. Y. Fan, X. L. Wu, H. X. Li, H. W. Liu, G. G. Siu, and P. K. Chu, Appl. Phys. Lett. **88**, 041909 (2006).
[23] J. Y. Fan, H. X. Li, J. Iiang, L. K. Y. So, Y. W. Lam, and P. K. Chu, Small **4**, 1058 (2008).
[24] J. Wang, S. J. Xiong, X. L. Wu, T. H. Li, and P. K. Chu, Nano Lett. **10**, 1466 (2010).
[25] J. Zhu, Z. Liu, X. L. Wu, L. L. Xu, W. C. Zhang, and P. K. Chu, Nanotechnology **18**, 365603 (2007).
[26] X. L. Wu, S. J. Xiong, J. Zhu, J. Wang, J. C. Shen, and P. K. Chu, Nano Lett. **9**, 4053 (2009).
[27] C. Y. He, X. L. Wu, J. C. Shen, and P. K. Chu, Nano Lett. **12**, 1545 (2012).
[28] Y. He, Z. H. Kang, Q. S. Li, C. H. A. Tsang, C. H. Fan, and S. T. Lee, Angew. Chem Int. Ed. **48**, 128 (2008).
[29] S. Sato and M. T. Swihart, Chem. Mater. **18**, 4083 (2006).
[30] M. Rosso-Vasic, E. Spruijt, B. van Lagen, L. De Cola, and H. Zuilhof, Small **4**, 1835 (2008).
[31] K. H. Lee, S. K. Lee, and K. S. Jeon, Appl. Surf. Sci. **255**, 4414 (2009).
[32] M. Rosso, M. Giesbers, A. Arafat, K. Schroen, and H. Zuilhof, Langmuir **25**, 2172 (2009).
[33] M. Rosso, A. Arafat, K. Schroen, M. Giesbers, C. S. Roper, R. Maboudian, and H. Zuilhof, Langmuir **24**, 4007 (2008).
[34] S. Kundu, Y. M. Wang, W. Xia, and M. Muhler, J. Phys. Chem. C **112**, 16869 (2008).
[35] J. D. Holmes, K. J. Ziegler, R. C. Doty, L. E. Pell, K. P. Johnston, and B. A. Korgel, J. Am. Chem. Soc. **123**, 3743 (2001).
[36] R. Huang, H. Dong, D. Wang, K. Chen, X. Wang, J. Xu, and Z. Ma, Appl. Phys. Lett. **92**, 181106 (2008).
[37] J. Warga, R. Li, S. N. Basu, and L. Dal Negro, Appl. Phys. Lett. **93**, 151116 (2008).